PAPER

Spatial mode discriminator based on leaky waveguides

IOP Publishing Journal of Optics
J. Opt. **20** (2018) 065801 (6pp) https://doi.org/10.1088/2040-8986/aabc65

Spatial mode discriminator based on leaky waveguides

Jing Xu[1,2], Jialing Liu[1], Hongkang Shi[1] and Yuntian Chen[1,2]

[1] School of Optical and Electronic Information, Huazhong University of Science and Technology, Wuhan 430074, People's Republic of China
[2] Wuhan National Laboratory of Optoelectronics, Huazhong University of Science and Technology, Wuhan 430074, People's Republic of China

E-mail: yuntian@hust.edu.cn

Received 25 December 2017, revised 12 March 2018
Accepted for publication 9 April 2018
Published 4 May 2018

Abstract

We propose a conceptually simple and experimentally compatible configuration to discriminate the spatial mode based on leaky waveguides, which are inserted in-between the transmission link. The essence of such a spatial mode discriminator is to introduce the leakage of the power flux on purpose for detection. Importantly, the leaky angle of each individual spatial mode with respect to the propagation direction are different for non-degenerated modes, while the radiation patterns of the degenerated spatial modes in the plane perpendicular to the propagation direction are also distinguishable. Based on these two facts, we illustrate the operation principle of the spatial mode discriminators via two concrete examples; a w-type slab leaky waveguide without degeneracy, and a cylindrical leaky waveguide with degeneracy. The correlation between the leakage angle and the spatial mode distribution for a slab leaky waveguide, as well as differences between the in-plane radiation patterns of degenerated modes in a cylindrical leaky waveguide, are verified numerically and analytically. Such findings can be readily useful in discriminating the spatial modes for optical communication or optical sensing.

Keywords: spatial mode, mode discriminator, leaky waveguides

(Some figures may appear in colour only in the online journal)

1. Introduction

Optical fibers, as well as other different types of optical waveguides, are the backbone of our modern communication network, in which various degrees of freedom of light, i.e. frequency, polarization, and spatial modes, can be encoded to channel information. In particular, spatial mode division multiplexing (SDM) techniques that utilize spatial modes as information channels have been widely explored to increase the capacity of a single fiber [1] or waveguides in light of long-haul transmission or short distance connection [2]. Moreover, spatial modes are relevant in quantum information applications wherein the quantum states are encoded. In those applications, analysis and discrimination of different modal components are of crucial importance, i.e. the characterization of modal cross-talks in SDM or measurement of quantum states.

Spatial mode discrimination can be classified into in-line or off-line detection, depending on whether or not the light transmission is terminated. In-line spatial mode discrimination contains two steps: (1) tapping part of the light out of the target waveguide, and (2) the off-line detection, i.e. measuring the modal contents of light that is tapped from the target waveguide. In this regard, multimode couplers might be suitable for such a purpose, where the light at one of the outputs can be used for transmission and the rest of the outputs for off-line mode discrimination. The major drawback associated with multimode couplers is that the modal properties of the guided modes in the input and output of the multimode coupler are not preserved except when special effort is made [3]. Subsequently, the modal contents can be further analysed using a few off-line detection techniques, including grating structures [4] and mode demultiplexers [5–9]. In either grating or demultiplexer structures, the phase

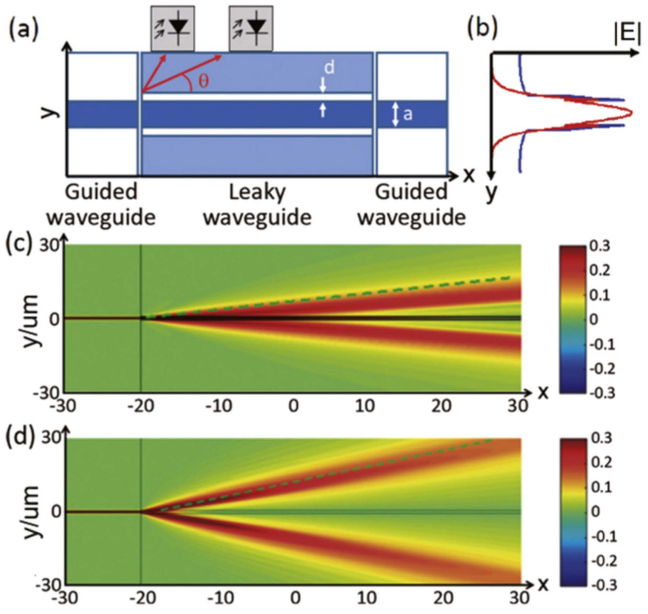

Figure 1. (a) Mode detection based on inserting a section of leaky waveguide between guided waveguides. (b) Modal profile of the normalized electrical field of the leaky (blue line) and guided (red line) waveguides in the core region; (c)–(d) show leaky mode excitation and propagation by placing a guided slab waveguide in front of a section of W-type slab waveguide. The TM0 and TM1 modes are excited in (c) and (d), respectively. Green dashed lines (c)–(d) are the predicted results by Monticone [19].

matching condition needs to be satisfied, which is not flexible to detect different modes once the grating or demultiplexer is fabricated.

Interestingly, leaky waveguides allow light to escape from the core into the cladding region, and potentially can be used to extract the information that is hidden inside the core of the waveguides, if the targeted waveguide and the leaky waveguide are well matched, such that the spatial mode can propagate through. Moreover, the field amplitude in the cladding region of the leaky waveguide mode grows exponentially in the transverse plane as light propagates, which leads to the possibility of distinguishing the spatial modes by monitoring the field in the cladding regions. Besides, it is found that leaky modes are of fundamental interest in sensing and coupling, due to their inherent properties of energy leaking [10–12], which can be used to tailor the radiation, guidance and filtering properties of different devices [13–16]. In this paper, we propose spatial mode discriminators to distinguish the spatial modes by resolving the angle of the leaked power flux of leaky waveguides inserted in-between the targeted waveguides, which support the certain guided modes under study; see figure 1(a).

2. Operation principle of mode descriminator

The underlying principle of the mode discriminators works as follows: (1) a section of the leaky waveguide is inserted into the link channel which contains several spatial modes that need to be distinguished, i.e. spatial modes propagating in a multimode waveguide, with the refractive indices of the core and cladding being n_1 and n_0 ($n_1 > n_0$). The leaky waveguide considered here has a w-profile of the refractive index, i.e. core, air gap and two cladding layers, with the refractive index being n_1, n_0 and n_1. (2) The inserted leaky waveguide has exactly the same geometry and profile of the refractive indices near the core region, thus the same spatial mode can be excited at the interface between the leaky waveguide and guided waveguide through the end-fire coupling. (3) After the excitation, the spatial modes excited inside the leaky waveguide propagate with different velocities and lossy rates, implying different leakage angles, see θ shown in figure 1(a), during the propagation along the inserted leaky guide. (4) The leaky angle θ can be resolved by placing photo-detectors at different longitudinal locations, thus different spatial modes can be distinguished. (5) For the waveguide mode with continuous or discrete symmetry in the cross-section, the polarization degeneracy may exist. For instance, one notes that the even and odd modes with mode label $(m, l) = (1, 1)$ correspond to two orthogonal polarization modes in cylindrical waveguides, and a pair of vector modes with spatial dependent polarizations for larger (m, l), which are coined as the polarization degeneracy onwards in this paper. Such polarization degeneracy can be further distinguished by studying the in-plane far-field distribution around the cladding, which will be discussed later. The width of the air gap in the leaky waveguide can be taken as control parameters to tune the leaky rate and propagation velocity, the leaky angle θ can be adjusted as desired. To illustrate how the proposed mode discriminator works, we provide two concrete examples, i.e. a two-dimensional (2D) slab waveguide and a three-dimensional circular waveguide, showing that the spatial modes indeed can be distinguished by monitoring the far-field distribution, even under the polarization degeneracy.

Firstly, we consider the coupling between the guided slab waveguide and the W-type leaky slab waveguide, in which the TE and TM modes are usually not degenerated, indicating all the modes in principle can be distinguished by identifying the propagation constants. A section of leaky waveguide is inserted into guided waveguides, as shown in figure 1(a), in which light travels along the x-axis. The refractive index of the core/cladding of the guided waveguide is n_1/n_0 with $n_1 > n_0$. The W-type leaky waveguide has two cladding layers, where the refractive indices of the core and outer cladding are n_1 and that of the inner cladding is n_0. The inserted leaky waveguide is designed to match the guided waveguide, as shown in figure 1(b), where the y-axis indicates the position corresponding to the cross-section of the waveguide. The modal profile inside the core layer of the guided waveguide (red) is almost the same as that of the leaky waveguide (blue). Therefore, a large portion of light is coupled from the guided waveguide to the leaky waveguide. By controlling the thickness of the inner cladding layer of the leaky waveguide [17, 18], it is possible to engineer the leaky rate such that most of the light still remains in the core of the leaky waveguide, and eventually goes back to the guided waveguide again. Meanwhile, a small fraction of light leaked

Table 1. Longitudinal fields of leaky modes in w-type fibers.

	E_z	H_z
$r \leqslant a$	$\frac{k_{1\perp}^2}{k_1^2} A_e Q_m J_{ml}(ur)$	$\frac{k_{1\perp}^2 n_1}{Z_0 k_1^2} A_h Q_m J_{ml}(ur)$
$r \geqslant a$ & $r \leqslant b$	$\frac{k_{2\perp}^2}{k_2^2} Q_m \begin{bmatrix} B_e I_{ml}(wr) \\ + \\ C_e K_{ml}(wr) \end{bmatrix}$	$\frac{k_{2\perp}^2 n_2}{Z_0 k_2^2} Q_m \begin{bmatrix} B_h I_{ml}(wr) \\ + \\ C_h K_{ml}(wr) \end{bmatrix}$
$r \geqslant b$	$\frac{k_{3\perp}^2}{k_3^2} D_e Q_m H_{ml}^{(2)}(ur)$	$D_h \frac{k_{3\perp}^2 n_3}{Z_0 k_3^2} Q_m H_{ml}^{(2)}(ur)$

out from the leaky waveguide can be harvested to analyse the modal contents of the targeted waveguide.

As shown in figure 1(a), different spatial modes leak at different angles that are related to their propagation constants. In principle, one can detect the intensity of the light at different points parallel to the waveguide axis to find out the propagation constant of the corresponding spatial modes. As an example, the parameters of the guided and leaky waveguides are set to: $n_1 = 1.45$, $n_0 = 1$, $\lambda = 1\ \mu$m, $a = 1\ \mu$m, $d = 0.1\ \mu$m. We study the propagation of TM_0 and TM_1 modes in the leaky waveguide, as shown in figures 1(c) and (d). The modal indices of TM_0 and TM_1 of the guided waveguide are found to be 1.40 and 1.24, respectively [20]. The corresponding leaky angles predicted by Monticone *et al* [19], i.e. $\theta = tan^{-1}(Re[k_{1\perp}]/Re[\beta])$, are 15° and 31°, respectively, as shown by the dashed green lines in figures 1(c) and (d). Evidently, the spatial modes become distinguishable by using a 1D photo-detector array by monitoring the leaked light on the surface of the cladding region. Importantly, the fraction of the leaked power flux for detection is controllable by adjusting the length of the leaky guide and the leaky rate. In the ideal scenario, only a small fraction of the power is leaked for detection purposes, whereas the majority can propagate through the leaky part, leading to the spatial mode discriminator simply from the on-the-fly detection.

3. Mode discriminator with polarization degeneracy

We continue to discuss the discrimination of the spatial modes with polarization degeneracy by monitoring the in-plane far-field radiation patterns [21]. For simplicity, we consider the w-type leaky cylindrical waveguide that is matched with two circular waveguides. In the cylindrical coordinate, i.e $\boldsymbol{r} = (r, \theta, z)$, the longitudinal component of E/H field associated with W-type leaky waveguide, with the core radius a and inner cladding radius b, can be given in the form of a plane wave along the z-axis $e^{(j\omega t - j\beta z)}$ with complex modal profiles to be determined in the x-y plane. For self consistency, we tabulate the longitudinal field component of the hybrid mode in three regions, i.e. in table 1 for the cylindrical leaky waveguide [15, 16, 22]. In table 1, J_m is a Bessel function of the first kind, I_m/K_m is a modified Bessel function of the first/second kind, while $H_m^{(2)}$ Hankel is a function of second kind, where $k_i^2 = k_0^2 n_i^2 = \beta^2 + k_{i\perp}^2$, $u = \sqrt{n_i^2 k_0^2 - \beta^2}$, $w = \sqrt{\beta^2 - n_0^2 k_0^2}$, $Q_m = \begin{matrix}\cos \\ \sin\end{matrix}(m\phi)\ k_0/Z_0$ is vacuum wave-number/impedance, θ/r is azimuthal/radial coordinate, the indices m/l represent the azimuthal/radial mode labels, and n_i is refractive index in i layer. From field continuity, one can solve the characteristic equation, and determine the coefficients $[A_e, B_e, C_e, D_e, A_h, B_h, C_h, D_h]$ listed in table 1 to obtain the eigenfield. Table 2 summarizes the propagation constants of the leaky modes of a W-type waveguides, using the aforementioned semi-analytical method and finite element full-wave simulation in COMSOL [23]. As a benchmark, the results obtained from the two independent approaches agree well.

Table 2. The comparison of propagation constants calculated by analytical expression and FEM. Parameters used are $n_1 = 3.16$, $n_0 = 1$, $\lambda = 1\ \mu$m, $a = 700$ nm, $d = 50$ nm, $l = 1$.

m	β (analytical)	β (FEM)	θ
1	$3.00 - 4.52 \times 10^{-3} i$	$3.00 - 4.30 \times 10^{-3} i$	18.44°
2	$2.72 - 2.09 \times 10^{-2} i$	$2.72 - 2.11 \times 10^{-2} i$	30.68°
0	$2.67 - 1.66 \times 10^{-3} i$	$2.67 - 1.66 \times 10^{-3} i$	32.40°
0	$2.80 - 3.16 \times 10^{-2} i$	$2.80 - 3.11 \times 10^{-2} i$	27.72°

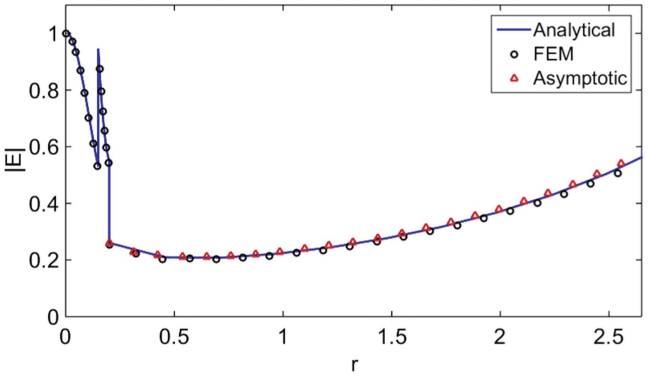

Figure 2. Normalized electrical field of the W-type cylindrical optical waveguides at $\phi = 0$ by three methods, i.e. analytical expression (blue line), FEM (black circles) and asymptotic expression (red triangles) with $m = 1$. The other parameters are the same as given in table 2.

As shown in table 1, the degenerated mode pair labelled by the same mode label (m, l), i.e. the even and odd modes, always exist due to the continuous rotation symmetry [24]. To distinguish the spatial modes with polarization degeneracy, we examine the asymptotic approximation of the electrical fields of the leaky modes. In the asymptotic approximation, we only need to consider the field profiles in the outer cladding region, i.e. $r \geqslant b$. Using the asymptotic expression for the Hankel function, one can find the asymptotic forms for the even/odd leaky modes of order m given as follows

$$\begin{pmatrix} E_z \\ E_\rho \\ E_\phi \end{pmatrix} = \sqrt{\frac{8}{\pi x k_3^4}}\, e^{j\left(\frac{(1+2m)\pi}{4} - x\right)} \begin{pmatrix} k_{3\perp}^2 D_e F(m\phi) \\ juD_e \beta F(m\phi) \\ -juD_h k_3 G(m\phi) \end{pmatrix}, \quad (1)$$

where $x = ur$, $F(m\phi) = \begin{matrix} j\sin \\ \cos \end{matrix}(m\phi)$ $(G(m\phi) = \begin{matrix} \cos \\ j\sin \end{matrix}(m\phi))$ depending on whether m is even or odd. Figure 2 shows the field amplitude as a function of r at $\phi = 0$, calculated by using asymptotic approximation (red triangles), analytical

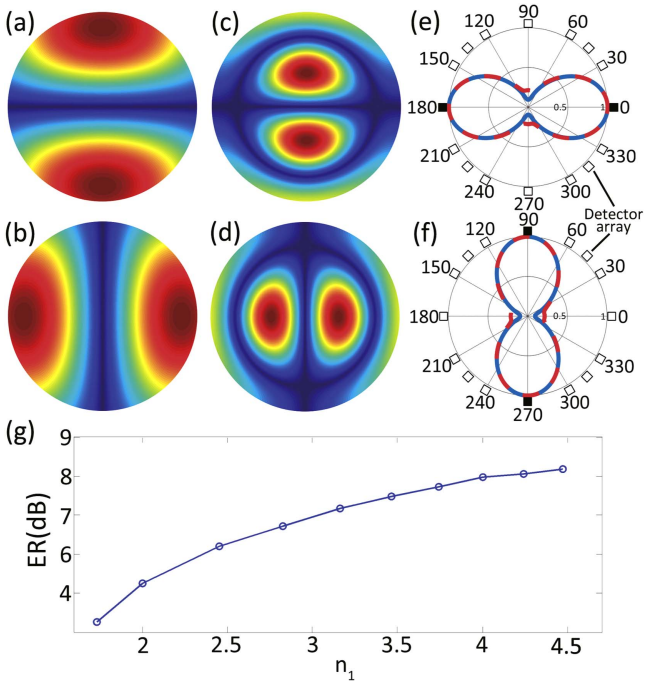

Figure 3. $|E_z|$ of the even leaky modes of the core region with $(m, l) = (1, 1/2)$ in (a), (c), and $|E_z|$ of odd leaky mode with $(m, l) = (1, 1/2)$ in (b), (d). (e), (f) Far-field radiation patterns of (a), (b) (blue) and (c), (d) (red). (g) SNR of spatial mode discriminator for two degenerated modes as n_1 varies, while $n_0 = 1$. The other parameters are the same as given in table 2.

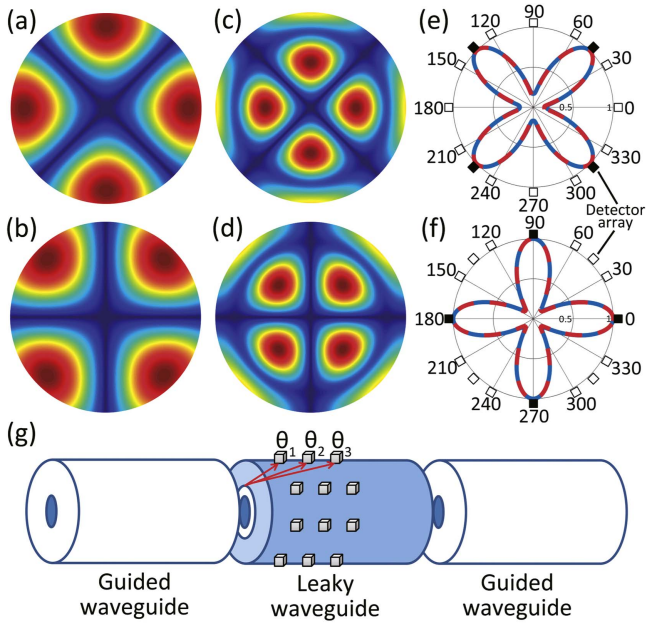

Figure 4. $|E_z|$ of the even leaky modes in the core region with $(m, l) = (2, 1/2)$ in (a), (c), $|E_z|$ of the odd leaky modes in the core region with $(m, l) = (2, 1/2)$ in (b), (d); (e), (f) far-field radiation patterns of (a), (b) (blue) and (c), (d) (red). (g) Structure of the spatial mode discriminator. The other parameters are the same as given in table 2.

expression (blue line) as well as full-wave finite element simulations using COMSOL [23] (black circles). It is clear that modal profiles calculated by the three methods match well with each other.

We now proceed to investigate the properties of the far-field radiation patterns using equation (1). The far-field patterns of the leaky modes in the *x*-*y* plane can be derived from asymptotic expressions divided by $e^{-jx}/\sqrt{x/u}$. We first analyse the degenerated fundamental leaky modes with $(m, l) = (1, 1 \text{ or } 2)$, with the two polarizations orthogonal to each other. Figures 3(a)–(d) show the $|E_z|$ component in the core region of the leaky waveguide, where figures 3(a) and (b) show the even/odd leaky modes of $(m, l) = (1, 1)$, while figures 3(c) and (d) shows the even/odd leaky modes of $(m, l) = (1, 2)$. The corresponding far-field radiation patterns are given in figures 3(e) and (f), where the blue solid line is for the even mode and odd mode with $(m, l) = (1, 1)$, while red dashed line is for the even mode and odd mode with $(m, l) = (1, 2)$. It can be proved that the far-field radiation patterns are rotated by $\frac{\pi}{2m}$ between even and odd modes for fixed (m, l). Moreover, there is a strong correlation between the distribution of the leaky light in the azimuthal direction of the waveguide and the angle of radiation peaks. Therefore, it is possible to distinguish the two orthogonal polarized fundamental modes on the fly without affecting the transmission of the guided modes by using a 2D photo-detector array, which can detect the light intensity on the surface of the leaky waveguide. Also, the spark angle, i.e. the angular position of the detector which is fired or yields the largest output signal in the array, is related to the angle of radiation peaks, i.e. even modes at $\theta = (0, \pi)$, and odd modes at $\theta = \left(\frac{\pi}{2}, \frac{3\pi}{2}\right)$. In order to study the performance of the discriminator, it is necessary to examine the signal to noise ratio (SNR), defined as the value of the radiation peak divided by the radiation intensity of the partner mode at the same angle. As an example, the SNR of the mode pair with $(m, l) = (1, 1)$ can be extracted by dividing the far field intensity of odd modes at $\theta = \frac{\pi}{2}$ by the far field intensity of the even mode at the same angle, as shown in figure 3(f), in which n_1 varies and n_0 is constant. It can be seen that SNR increases for larger values of $|n_1 - n_0|$, indicating that a large index contrast provides a better SNR. It is worthy to point out that the working principle of distinguishing the lowest degenerated mode pair can be extended to other high order mode pairs.

Indeed, figure 4 analyses the high-order modes with $(m, l) = (2, 1)$ and $(m, l) = (2, 2)$. Figures 4(a)–(d) show $|E_z|$ in the core region of the leaky waveguide. As can been seen, figures 4(a) and (b) show the even/odd leaky modes of $(m, l) = (2, 1)$, while figures 4(c) and(d) show the even/odd leaky modes of $(m, l) = (2, 2)$. The corresponding far-field radiation patterns are shown in figures 4(e) and (f), with blue lines for $l = 1$ and red dashed lines for $l = 2$. It can be seen that the far-field radiation patterns are rotated by $\pi/4$ between the even and odd modes for fixed (m, l). Evidently, there is a strong correlation between the near field distribution along the azimuthal direction and far-field patterns of the leaky modes, similar to that of the degenerated fundamental leaky modes. Therefore, the 2D photo-detector array to detect the far-field intensity can be placed at the proper angle with respect to the *z*-axis on the surface of the leaky waveguide for high-order

mode discrimination. Meanwhile, it can be seen that modes with the same azimuthal mode label m but a different radial mode label l have similar radiation patterns. However, the propagation constants of those modes with the same m are different, leading to different leaky angles that shall be taken into account to position the detector arrays. In brief, the leaky angles shown in figure 4(g), i.e. θ_1, θ_2, θ_3, are essentially given by the propagation constants, which are different for different (m, l), similar to to discussions in figure 1. For the two degenerated modes with the same (m, l), the two modes can be distinguished by using the in-plane detector array, as sketched in figures 4(e) and (f).

As we can see from figure 4(g), the spatial mode discriminator based on leaky waveguides is composed of two guided waveguides, a leaky waveguide and an array of in-plane detectors. The cores of the two guided waveguides and the leaky waveguide have the same size and the same effective refractive index. The detector array is arranged on the surface of the leaky waveguide and is composed of a plurality of detectors of the same performance arranged radially around the leaky mode waveguide. The following points will support the fabrication of our spatial mode discriminator: (1) the method of fabricating a leaky waveguide is the same as that of an ordinary waveguide, (2) the existing waveguide docking technologies are very mature, and (3) there are many detectors such as graphene detectors that can match the size of our waveguides. Therefore, with the support of technology and theory, we will discuss the experiment and the fabrication of the spatial mode discriminator based on leaky waveguides in our future work.

4. Conclusion

In closing, we propose a conceptually simple approach to discriminate spatial modes in waveguides, validated by semi-analytical calculations and finite element fullwave simulations. The key component in our spatial waveguide discriminator is the leaky waveguides inserted in-between two normal waveguides, wherein the same spatial mode is coupled from the first normal guide to the leaky guide, and eventually to the second normal guide. The purpose of the leaky waveguide is to introduce a certain leakage of the power flux of the spatial mode for detection. Importantly, the leaky angles show strong correlations with the spatial modes. For a waveguide without mode degeneracy, we show that the leaky angles for different spatial modes are different, thus can be distinguished by detecting the leaked power flux on the surface of the outer-cladding region. For a waveguide with mode degeneracy, we show that the in-plane radiation patterns of the two degenerated spatial modes are different, thus can also be distinguished by placing the detector array in the plane at the proper leaky angle.

Compared with the general in-line spatial mode discrimination such as multimode couplers, the spatial mode discriminator based on leaky waveguides preserves the modal profiles of the guided modes in the input and output and ensures the integrity of the modal transmission of the signal. At the same time, compared with the existing off-line detection techniques, including grating structures and mode demultiplexers, our spatial mode discriminator can realize modal analysis on the fly without affecting modal transmission. In addition, leaky waveguides match the guided waveguide as long as their cores have the same size and the same effective refractive index as the core of guided waveguide, which is more flexible than using grating structures or mode demultiplexers to detect different modes. We believe this work will be widely used in sensing, optical communications in the future.

Funding

This work was supported in part by National Natural Science Foundation of China (Grant Nos. 61405066, 61405067, 61775063 and 61735006), National Key Research and Development Program of China (Grant No. 2017YFA0305200), and the Fundamental Research Funds for the Central Universities, HUST: 2017KFYXJJ027.

ORCID iDs

Jialing Liu https://orcid.org/0000-0001-6393-6197

References

[1] Richardson D J, Fini J M and Nelson L E 2013 Space-division multiplexing in optical fibers *Nat. Photonics* **7** 354
[2] Wang J, He S and Dai D 2014 On-chip silicon 8-channel hybrid (de)multiplexer enabling simultaneous mode- and polarization-division-multiplexing *Laser Photon. Rev.* **8** L18
[3] Mori T, Sakamoto T, Yamamoto T and Tomita S 2011 Coherent optical MIMO transmission over 20 km GI multimode fiber by using digital coherent receiver with mode convergence unit *Opt. Express* **19** 16252
[4] Al Amin A, Li A, Chen S, Chen X, Gao G and Shieh W 2011 Dual-LP 11 mode 4x4 MIMO-OFDM transmission over a two-mode fiber *Opt. Express* **19** 16672
[5] Hanzawa N, Saitoh K, Sakamoto T, Matsui T, Tsujikawa K, Koshiba M and Yamamoto F 2014 Mode multi/demultiplexing with parallel waveguide for mode division multiplexed transmission *Opt. Express* **22** 29321
[6] Ding Y *et al* 2013 On-chip two-mode division multiplexing using tapered directional coupler-based mode multiplexer and demultiplexer *Opt. Express* **21** 10376–82
[7] Li A, Chen X, Al Amin A and Shieh W 2012 Fused fiber mode couplers for few-mode transmission *IEEE Photon. Technol. Lett.* **24** 1953–6
[8] Dong J, Chiang K S and Jin W 2015 Compact three-dimensional polymer waveguide mode multiplexer *J. Lightwave Technol.* **33** 4580–8
[9] Gross S, Riesen N, Love J D and Withford M J 2014 Three-dimensional ultra-broadband integrated tapered mode multiplexers *Laser Photon. Rev.* **8** L18–85
[10] Shenoy M R, Thyagarajan K and Ghatak A K 1988 Numerical analysis of optical fibers using matrix approach *J. Lightwave Technol.* **6** 1285–91
[11] Sun N H, Butler J K, Evans G A, Pang L and Congdon P 1997 Analysis of grating-assisted directional couplers using the Floquet-Bloch theory *J. Lightwave Technol.* **15** 2301–15

[12] Yang H, Li Q and Qiu M 2016 Identification and control of multiple leaky plasmon modes in silver nanowires *Laser Photon. Rev.* **10** 278–86
[13] Snyder A W and Mitchell D J 1974 Leaky mode analysis of circular optical waveguides *Opto-electronics (London)* **6** 287–96
[14] Kawakami S and Nishida S 1974 Characteristics of a doubly clad optical fiber with a low-index inner cladding *IEEE J. Quantum Electron.* **10** 879–87
[15] Kawakami S and Nishida S 1975 Perturbation theory of a doubly clad optical fiber with a low-index inner cladding *IEEE J. Quantum Electron.* **11** 130–8
[16] Maeda M and Yamada S 1977 Leaky modes on W-fibers: mode structure and attenuation *Appl. Opt.* **16** 2198–203
[17] Sun N H, Chou C C, Chang H W, Butler J K and Evans G A 2006 Radiation loss of grating-assisted directional couplers using the Floquet-Bloch theory *J. Lightwave Technol.* **24** 2409–15
[18] Renner H 1991 Leaky-mode loss in coated depressed-cladding fibers *IEEE Photon. Technol. Lett.* **3** 31–2
[19] Monticone F and Alù A 2015 Leaky-wave theory, techniques, and applications: from microwaves to visible frequencies *Proc. IEEE* **103** 793–821
[20] Hu J and Menyuk C R 2009 Understanding leaky modes: slab waveguide revisited *Adv. Opt. Photonics* **1** 58–106
[21] Chou C C and Sun N H 2008 Analysis of leaky-mode losses for optical fibers *J. Opt. Soc. Am.* B **25** 545–54
[22] Lee S L, Chung Y, Coldren L A and Dagli N 1995 On leaky mode approximations for modal expansion in multilayer open waveguides *IEEE J. Quantum Electron.* **31** 1790–802
[23] COMSOL http://comsol.com/
[24] Xiong Z F, Chen W J, Wang P and Chen Y T 2017 Classification of symmetry properties of waveguide modes in presence of gain/losses, anisotropy/bianisotropy, or continuous/discrete rotational symmetry *Opt. Express* **25** 29822–34